Chem. Res. Chin. Univ., 2016, 32(1), 106—111 doi: 10.1007/s40242-016-5277-5

Dealloyed Silver Nanoparticles as Efficient Catalyst Towards Oxygen Reduction in Alkaline Solution

CUI Qinghua[1,2], ZHANG Yelong[1,2] and PENG Zhangquan[1*]

1. State Key Laboratory of Electroanalytical Chemistry, Changchun Institute of Applied Chemistry, Chinese Academy of Sciences, Changchun 130022, P. R. China;

2. University of Chinese Academy of Sciences, Beijing 100049, P. R. China

Abstract Silver nanoparticles(Ag NPs) were prepared by dealloying Mg-Ag alloy precursor. The obtained Ag NPs have an average ligament size of (50±10) nm. Electrocatalytic activity of Ag NPs towards oxygen reduction reaction(ORR) in 0.1 mol/L NaOH solution was assessed *via* cyclic voltammetry(CV), rotating ring disk electrode(RRDE) techniques, and electrochemical impedance spectroscopy(EIS). The electrochemical active area for the ORR was evaluated by means of the charge of the underpotential deposition(UPD) of lead(Pb) on Ag NPs. The CV results indicate that Ag NPs have a higher current density and more positive onset potential than the bulk Ag electrode. RRDE was employed to determine kinetic parameters for O_2 reduction. Ag NPs exhibit a higher kinetic current density of 25.84 mA/cm^2 and a rate constant of 5.45×10^{-2} cm/s at –0.35 V *vs*. Hg/HgO. The number of electrons(n) involved in ORR is close to 4. Further, EIS data show significantly low charge transfer resistances on the Ag NPs electrode. The results indicate that the prepared Ag NPs have a high activity and are promising catalyst for ORR in alkaline solution.

Keywords Silver nanoparticles; Electrochemical activity; Oxygen reduction reaction

1 Introduction

The ever-increasing demands for fossil fuels worldwide, coupled with the limited reserves in nature, have motivated significant investigations for exploring renewable and sustainable sources of energy[1—4]. Today, proton exchange membrane fuel cells(PEMFCs) and metal-air batteries have been playing an important role in our sustainable development society because they bring about generated renewable energy[5—7]. For such application, one of the limits is the electrochemical over potentials for oxygen reduction reaction(ORR) at the cathode[2]. In order to accelerate the ORR rate to meet a practical application, the catalysts for ORR are therefore needed to be developed. Many efforts have been devoted to the studies on ORR catalysts, in which those based on platinum(Pt) are considered to be the most effective[8—10]. However, its high cost and rare storage in earth have limited its commercial applications for fuel cells. Developing alternative catalysts has become a necessity that have been intensively investigated during the past decades. These alternative catalysts include noble metals and their alloys, transition metals and their compounds, carbon materials, quinone and its derivatives[11—15].

Among these various candidates, silver(Ag) is a promising alternative catalyst because of its abundance in nature and low cost, especially its high catalytic activity towards ORR in alkaline media[16,17] For example, Demarconnay *et al*.[18] reported that the onset potential of 20% Ag/C showed a negative shift of 50 mV for ORR compared to that of Pt/C catalyst. Ag-based catalyst or Ag nanoparticles(Ag NPs) supported on carbon(C) have extensive application for alkaline fuel cells[19—22].

The catalytic activity of Ag NPs toward ORR in alkaline media was investigated. The Ag NPs catalysts, prepared by dealloying Mg-Ag alloy precursor, were characterized by X-ray diffraction(XRD) and scanning electron microscopy(SEM). Its electrochemical catalytic activity toward ORR in alkaline electrolyte was studied by cyclic voltammetry(CV), rotating ring disk electrode(RRDE) measurements, and electrochemical impedance spectroscopy(EIS). The kinetics, electron transfer number(n) and the exchange current density(j_0) were analyzed with steady-state polarization data from RRDE.

2 Experimental

2.1 Ag NPs Preparation

The precursor ingot with a nominal composition of $Mg_{77}Ag_{23}$ was firstly prepared by alloying pure Mg and Ag(99.9%) in a resistance furnace under the protection of covering fluxes[23]. Subsequently, it was remelted in a quartz tube using high-frequency induction heating in a single roller melt spinning apparatus and rapidly solidified into ribbons(thickness 20—50 m and width 2—5 mm) under an argon protection. To obtain the Ag nanoparticles(Ag NPs), the $Mg_{77}Ag_{23}$ ribbons were dealloyed in a 1%(mass fraction) hydrochloric acid solution for 10 min. The as-dealloyed sample was washed with deionized(DI) water and dehydrated ethanol several times. Prior to electrochemical measurement, Ag NPs were ground to

*Corresponding author. E-mail: zqpeng@ciac.ac.cn

Received July 17, 2015; accepted August 13, 2015.

Supported by the Strategic Priority Research Program of the Chinese Academy of Sciences(No.XDA09010401).

powder with a mortar and pestle.

2.2 Characterization

Powder X-ray diffraction patterns were obtained on a D/Max 2500 V/PC Powder Diffractometer using Cu *Kα* radiation. The morphology and microstructure were characterized with a XL30 scanning electron microscope. The chemical compositions of the as-prepared sample were determined on an energy-dispersive X-ray(EDX) analyzer attached to an SEM.

2.3 Electrochemical Measurements

All the electrochemical experiment were performed in a standard three-electrode electrochemical cell with the help of a CHI 760E Potentiostat. A plate-like Pt counter electrode and a Hg/HgO reference electrode were used in all the electrochemical measurement. The working electrode for cycle voltammetry was a silver disk electrode(Ag, 2 mm in diameter) and a catalysts-coated glass carbon electrode(GC, 3 mm in diameter). The RRDE electrode was composed of a catalyst-deposited glassy carbon disk(5.16 mm in diameter) surrounded by a Pt ring to sense the HO_2^- produced at the working disk electrode. The electro-catalytic activities of Ag NPs for ORR were measured by virtue of an MSR rotating ring disk electrode (Pine). The electrocatalytic ink was prepared by dispersed Ag NPs/carbon XC-72(1:3, mass ratio) in a mixture of water, isopropyl alcohol, and 5%(mass fraction) Nafion(4:1:0.05, volume ratio) to reach a concentration of 1 mg/mL and sonicated for 30 min. Then a certain amount of the catalyst ink was cast on prepolished glassy carbon electrode for CV measurmentand and RRDE electrode for steady-state polarization measurement, yielding a catalyst powder loading of 4 and 20 μg, respectively. Prior to ORR measurement, the catalyst electrodes(Ag NPs/C) were cleaned first using CV in a range of –0.3 to 0.3 V(*vs*. Hg/HgO) in a N_2-saturated 0.5 mol/L NaCl solution and then in the range of –0.6 to 0.2 V(*vs*. Hg/HgO) in a N_2-saturated 0.1 mol/L NaOH solution[24,25]. All the ORR measurement was performed in a O_2-saturated 0.1 mol/L NaOH solution. The disk rotation rate of RRDE was set at 400, 800, 1200 and 1600 r/min at a scanning rate of 5 mV/s. Current densities of Ag electrode for ORR were calculated according to its geometric surface area, whereas the current densities of Ag NPs modified electrode was obtained from the electrochemical surface area derived from underpotential deposition(UPD) of Pb on the Ag NPs surface(see below). Electrochemical impedance spectroscopy(EIS) was implemented in a frequency range from 100 kHz to 10 mHz at –0.2 V *vs*. Hg/HgO with 5 mV amplitude.

2.4 Electrochemical Surface Area Determination

The UPD of Pb on Ag NPs was employed to determine the electrochemical accessible surface area for ORR[24—28]. The UPD process was carried out on Ag NPs/C modified GC electrode in a solution of 5 mmol/L lead perchlorate [$Pb(ClO_4)_2$, Sigma-Aldrich], 10 mmol/L perchloric acid($HClO_4$, Sigma-Aldrich, 70%, volume fraction) and 0.1 mol/L sodium perchlorate($NaClO_4$, Sigma-Aldrich). The true Ag NPs surface area was calculated from the area under the Pb UPD stripping peak based on the theoretical value of Pb UPD surface charge of 260 μC/cm^2[28]. This obtained available area was used to evaluate the current density per unit area of the Ag NPs in CV and RRDE.

3 Results and Discussion

3.1 Characteristics of Ag NPs

Fig.1(A) shows the XRD patterns of the as-dealloyed sample. The diffraction peaks can be indexed to Ag(PDF No.65-2871), no other distinguishable diffraction peaks can be detected. The SEM image shows the morphology and microstructure of the Ag NPs. As illustrated in Fig.1(B), the resulting nanostructures with an open-cell structure and nanosized ligaments are clearly observed. The as-prepared Ag NPs have an average ligament size of (50±10) nm. Moreover, the self-similar three-dimensional bicontinuous interpenetrating ligament-channel structure may largely facilitate the mass transfer fluxes and greatly reduce electron and mass transfer resistance, which are beneficial to the improvement of electrochemical activity. The EDX spectrum[Fig.1(C)] shows that the predominant component is Ag, which is in agreement with the

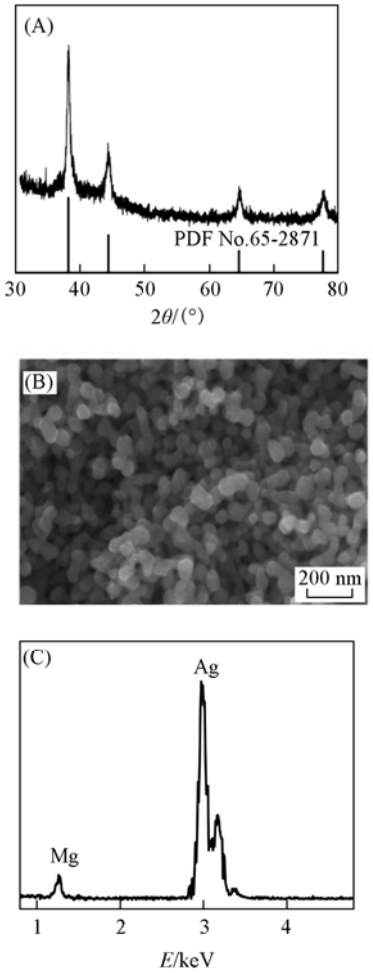

Fig.1 XRD pattern(A), SEM image(B) and the corresponding EDX spectrum(C) of the as-prepared Ag NPs

XRD analysis. Although Mg has been etched out of the precursor on a large scale, there is still 3.5%(molar fraction) residual Mg can be detected in Ag NPs. This suggests that the yield of Ag NPs prepared by dealloying $Mg_{77}Ag_{23}$ is 96.5%(molar fraction) in the present investigation.

3.2 Electrocatalytic Activity of Ag NPs Towards ORR in Alkaline Medium

To completely remove the residual Mg and clean the catalyst of Ag NPs/C film, CV was carried out in the range of –0.3—0.3 V(*vs*. Hg/HgO) in a N_2-saturated 0.5 mol/L NaCl solution and then in a range of –0.6—0.2 V(*vs*. Hg/HgO) in a N_2-saturated 0.1 mol/L NaOH solution[24,25]. It should be noted that the Ag NPs modified electrode cycled in a N_2-saturated 0.5 mol/L NaCl solution can remove the residual Mg in the Ag NPs. As shown in Fig.2(A), the catalyst has a pair of sharp redox current peaks in a N_2-saturated 0.5 mol/L NaCl solution, the anodic peak at 0.109 V and a cathodic peak at –0.06 V. Ag in the Ag NPs is electro-oxidated to AgCl in the positive scan, and this process is reversed in the negative scan. The cycle of Ag/AgCl corresponds to a solid-state phase transformation from Ag NPs to AgCl NPs. This dissolution and redeposition process of Ag NPs would release the impurities in Ag NPs. It was confirmed by the disappearance of the Mg signal at 1.27 keV in EDX spectrum[Fig.2(B)] of Ag NPs/C film. All the signals of C, O, F and S are from the binder Nafion in the film, except for the signal of Si that is from the substrate that supported the sample.

The electrochemical surface area of Ag NPs in Ag NPs modified GC electrode was obtained by the method of Pb

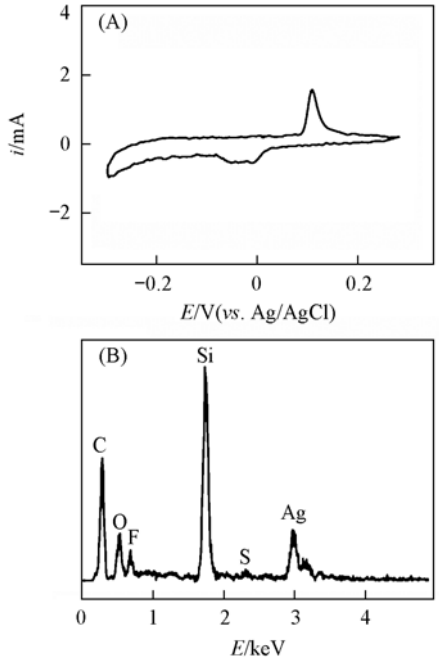

Fig.2 CV of Ag NPs modified electrode in N_2-saturated 0.5 mol/L NaCl before ORR measurement(A) and EDX spectrum for Ag NPs/C film(B)

(A) Scan rate: 50 mV/s.

UPD[24,26—28]. Fig.3 shows the typical Pb UPD cyclic diagram on a bulk Ag electrode and Ag NPs modified GC electrode surface. The cathodic peak at –0.387 V and anodic peak at –0.354 V correspond to the deposition and removal of the Pb on the surface of Ag NPs, in agreement with previous reports. Based on the theoretical value of 260 μC/cm^2 for Pb UPD charge on Ag, the calculated electrochemical area of Ag NPs in Ag NPs/C film is 0.018 cm^2. The same process was done for the Ag NPs modified RRDE electrode.

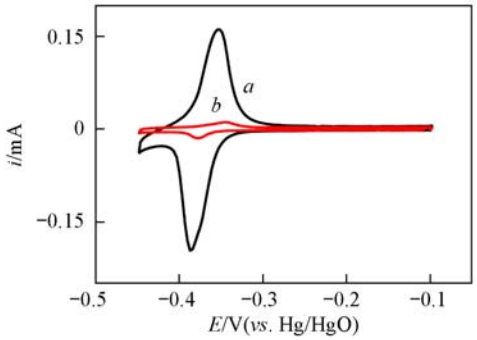

Fig.3 Underpotential deposition of Pb on bulk Ag electrode(*a*) and Ag NPs modified GC electrode(*b*) in 5 mmol/L $PbCl_2$+10 mmol/L $HClO_4$+0.1 mol/L $NaClO_4$ solution

Scan rate: 50 mV/s.

The electro-catalytic activity of Ag NPs was first studied on the Ag NPs modified GC electrode in 0.1 mol/L NaOH saturated with O_2. Fig.4 compares the CV curves of Ag electrode and the Ag NPs modified GC electrode towards ORR. The onset potential at Ag NPs modified electrode is –0.07 V, showing an positive shift of 60 mV compared to that of bulk Ag electrode(–0.13 V). The electrochemical surface area-normalized current densitiy of Ag NPs is 7.95 mA/cm^2, which is almost *ca*. 5 times that of Ag electrode(1.697 mA/cm^2). Results reveal that the Ag NPs exhibit a better catalytic activity for ORR than bulk Ag electrode.

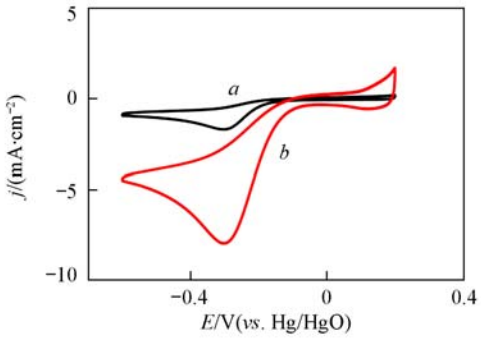

Fig.4 CV curves for O_2 reduction on bulk Ag electrode(*a*) and the Ag NPs modified GC electrode(*b*) in 0.1 mol/L NaOH saturated with O_2

Scan rate: 0.1 V/s.

To investigate the kinetics of Ag NPs towards ORR, we carried out a RRDE measurement in 0.1 mol/L NaOH(Fig.5). The current corresponding to HO_2^- oxidation is recorded by the ring electrode[Fig.5(A)]. Fig.5(B) gives the typical current-potential curves for ORR of Ag NPs modified glass carbon disk electrode at different rotation rates. The electron transfer number(*n*) per O_2 molecule is very important for investigating

ORR pathway. The HO_2^- generation should be considered due to its damage to the electrolyte membrane of alkaline fuel cells(AFCs)[29,30]. The electron transfer number and percentage(%) of HO_2^- generated during the ORR process can be calculated according to Eqs.(1) and (2), respectively.

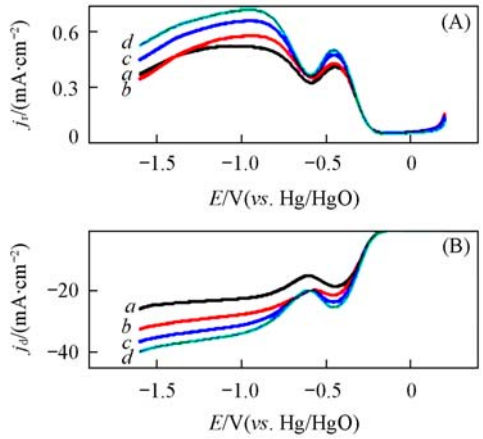

Fig.5 RRDE measurement for HO_2^- reoxidation on Pt ring electrode(A) and ORR on Ag NPs modified glass carbon disk electrode(B)

Rotation rate/(r·min^{-1}): *a*. 400; *b*. 800; *c*. 1200; *d*. 1600.

$$n = i_d / (i_d + i_r/N) \quad (1)$$

$$HO_2^- \text{ yield}(\%) = \frac{2i_r/N}{i_d + (i_r/N)} \times 100\% \quad (2)$$

where i_d is the disk current; i_r is the ring current and N is the collection efficiency. The calculated n values and the corresponding HO_2^- yield are presented in Fig.6. As shown in Fig.6, the HO_2^- yield during ORR is 4.87%—10.47% at a Ag NPs/C modified electrode in a potential range of –1.60 to –0.20 V, giving an electron transfer number of 3.80—3.91[Fig.6(B)]. The electron transfer number at Ag NPs/C modified electrode is higher than that of the Ag catalysts prepared *via* a colloidal method or a chemical reduction route. For example, the Ag/C catalyst with 20%(mass fraction) Ag on carbon was prepared using a colloidal route by Demarconnay *et al.*[18], with a particle size close to 15 nm. The electron transfer number is only close to 3.5—3.7, whatever the potential is. Adenosine 5′-triphosphate capped silver nanoparticles(ATP-Ag NPs) with

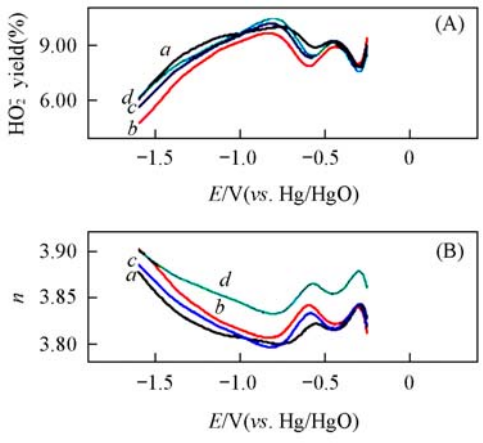

Fig.6 Peroxide yield(A) and electron transfer number(*n*)(B) calculated from the RRDE data

Rotation rate/(r·min^{-1}): *a*. 400; *b*. 800; *c*. 1200; *d*. 1600.

diameters of (4.5±1.1) nm were synthesized *via* a one-pot chemical reduction route by Singh *et al.*[24]. After removal of the ATP capping ligands, the electrochemical activity of these NPs was studied, finding the electron transfer number of these Ag NPs was 3.7—3.8 at a potential of –0.5 to –0.6 V *vs.* Ag/AgCl/KCl (saturated)[24]. Therefore, the prepared Ag NPs by dealloying Mg-Ag alloy precusor in the present study have higher currents available because that the electron transfer number is close to 4.

It is well known that the kinetic current density(j_k) describes the rate of charge transfer of a catalyst and therefore, is a direct measure of the electro-catalyst activity. The catalyst activity of Ag NPs for ORR was further investigated according to the Koutecky-Levich Eq.(3)[31]:

$$\frac{1}{j} = \frac{1}{j_k} + \frac{1}{j_d} \quad (3)$$

$$j_k = nFkc_0 \quad (4)$$

$$j_d = 0.62nFD^{2/3}\nu^{-1/6}c_0\omega^{1/2} \quad (5)$$

where j is the measured current density; j_k is the kinetic current density; j_d is diffusion limited current density; k is the rate constant of O_2 reduction(potential dependent); n is the electron transfer number in the oxygen reduction reaction; F is the Faraday constant(96485 C/mol); ω is the rotation rate in the radian(rad/s), c_0 is the saturation concentration of dissolved O_2 in 0.1 mol/L NaOH at 1.01×10^5 Pa O_2 pressure(1.26×10^{-6} mol/cm^3)[20]; D_{O_2} is the diffusion coefficient of O_2(1.93×10^{-5} cm^2/s) in NaOH solution; ν is the kinematic viscosity of the solution(1.09×10^{-2} cm^2/s)[20].

The disk currents of Ag NPs at several rotation rates were used to construct Koutecky-Levich(K-L) plots for each potential. As shown in Fig.7, the K-L plots display a linear behavior at given potentials, but the intercepts and slopes vary as a function of potential. Table 1 shows the values of j_k and the corresponding rate constants at given potentials, which are much higher than thoes in the previous reports[12,18,24].

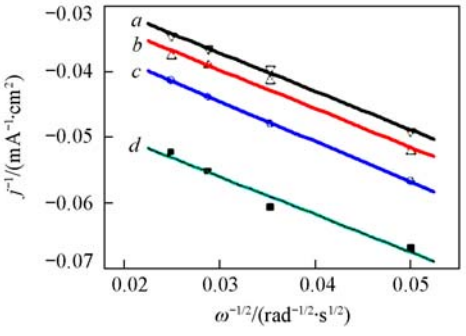

Fig.7 Koutecky-Levich plots for the AgNPs during ORR process

E/V: *a*. –0.35; *b*. –0.50; *c*. –0.75; *d*. –0.80.

Table 1 Kinetic analysis results for oxygen reduction reaction

E/V	–0.35	–0.50	–0.75	–0.80
j_k/(mA·cm^{-2})	25.84	38.24	45.49	51.26
10^2k/(cm·s^{-1})	5.45	8.06	9.59	10.81

Then, the kinetic analysis for the Tafel plot of ORR on Ag NPs was made(Fig.8) on the basis of mass-transport corrected current.

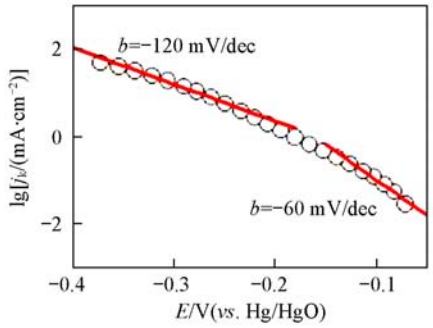

Fig.8 Tafel plots for the Ag NPs during ORR process at 1600 r/min

$$\lg|j_k| = \lg|j_0| + \frac{(1-\alpha)nF}{2.303RT}|\eta| \quad (6)$$

where j_k is the kinetic current density, obtained by correcting the measured current densities with diffusion, derived from Koutecky-Levich equation:

$$j_k = \frac{j \cdot j_d}{j_d - j} \quad (7)$$

The slope of Tafel plot varies with the potential, suggesting two slopes of –60 and –120 mV/dec at low and high current densities, respectively. This can be interpreted in terms of the different coverage of adsorbed oxygen at AgNPs/C film, *i.e.*, the Temkin isotherm at low overpotentials(high coverage) and the Langmuir isotherm at higher overpotentials(low coverage)[32—35]. From the Tafel intercept, we can obtain the exchange current density(j_0) of AgNPs/C(j_0=8.7×10^{-3} mA/cm^2), which is a little higher than that in previous report[18]. The results indicate that dealloyed Ag NPs are efficient catalyst for ORR.

In order to further investigate the electroactivity of the Ag NPs for ORR, the electrochemical impedance spectra(EIS) were measured at –0.2 V, and the results are presented in Fig.9. A kinetics-based model consisting of solution resistance(R_s), faradaic resistance(R_{ct}) and constant phase element(Q) was adopted to fit the impedance spectra. The parameters of the equivalent circuitare are listed in Table 2. Indeed, a sharp decrease in faradaic resistance for Ag NPs(331.7 Ω) could be observed compared to that in faradaic resistance for bulk Ag electrode(632.1 Ω), revealing its lower charge transfer resistance and higher catalytic activity toward the ORR. The outcome is in good agreement with the results from the RDE and Tafel measurements shown in Figs.5—8.

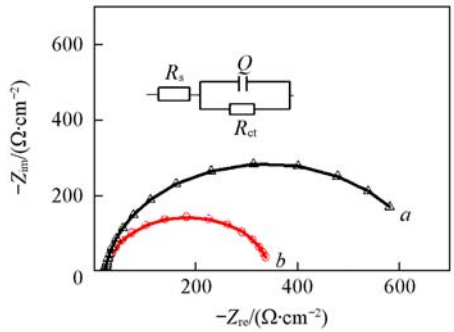

Fig.9 EIS of bulk Ag electrode(*a*) and the Ag NPs modified GC electrode(*b*) at –0.2 V *vs.* Hg/HgO in 0.1 mol/L NaOH saturated with O_2

The inset shows an equivalent electrical circuit consisting of the electrolyte resistance(R_s), interface charge transfer resistance(R_{ct}) and constant phase element(Q).

Table 2 Simulated elemental values of fitted equivalent circuit corresponding to the EIS spectra in Fig.9

Sample	R_s/(Ω·cm^{-2})	R_{ct}/(Ω·cm^{-2})	Q/(Ω^{-1}·cm^{-2}·S^n)	n
Ag electrode	20.8	632.1	0.0061	0.94
Ag NPs modified GC electrode	21.2	331.7	0.0048	0.84

From the above discussion, we believe that the good catalytic performance of the Ag NPs may be attributed to the following several aspects. Firstly, the three-dimensional metallic network of Ag NPs with excellent electrical conductivity could facilitate the electron transport. Secondly, the unique three-dimensional bicontinuous interpenetrating ligament-channel structure with good permeability for gas or liquid molecules can effectively decrease the mass transport resistance and facilitate high mass transfer fluxes, which might be beneficial to the improvement of catalytic activity for ORR. Thirdly, the high surface area may raise the quantity of exposed ORR active sites. Thus, all these advantages bring about the good electrocatalytic activity for ORR.

4 Conclusions

Ag NPs were prepared by dealloying Mg-Ag alloy precursor. It was electrochemically treated in a N_2-saturated NaCl solution to clean the impurities on Ag NPs surface. The electrochemical surface area of Ag NPs for ORR was evaluated by means of Pb UPD. Its catalytic activity for ORR was investigated by employing CV, RRDE and EIS in alkaline electrolyte. The Ag NPs have an electrochemical active area of 7.95 mA/cm^2, which is about 5 times that of bulk Ag electrode. Its onset potential positively shifted 60 mV compared to that of the bulk Ag electrode. RRDE results demonstrate that Ag NPs predominantly possess the direct four electron pathway and low HO_2^- produce. The results indicate that Ag NPs are promising and efficient catalyst for ORR.

References

[1] Borup R., Meyer J., Pivovar B., Kim Y. S., Mukundan R., Garland N., Myers D.,Wilson M., Garzon F., Wood D., Zelenary P., More K., Stroh K., Zawodzinski T., Macgrath J. E., Inaba M., Miyatake K., Hori M., Ota K., Ogumi Z., Miyata S., Nishikata A., Siroma Z., Uchimoto Y., Yasuda K., Kimijima K., Iwashita N., *Chem. Rev.*, **2007**, *107*(10), 3904

[2] Liang Y., Li Y., Wang H., Zhou J., Wang J., Regier T., Dai H., *Nat. Mater.*, **2011**, *10*(10), 780

[3] Liu M., Zhang R., Chen W., *Chem. Rev.*, **2014**, *114*(10), 5117

[4] Voiry D., Yamaguchi H., Li J., Silva R., Alves D. C. B., Fujita T., Chen M., Asefa T., Shenoy V. B., Eda G., Chhowalla M., *Nat. Mater.*, **2013**, *12*(9), 850

[5] Suntivich J., Gasteiger H. A., Yabuuchi N., Nakanishi H., Goodenough J. B., Yang S. H., *Nat. Chem.*, **2011**, *3*(7), 546

[6] Cui C. H., Li H. H., Yu J. W., Gao M. R., Yu S. H., *Angew. Chem. Int. Ed.*, **2010**, *49*(48), 9149

[7] Lu Y. C., Xu Z., Gasteiger H. A., Chen S., Hamad-Schifferli K., Yang

S. H., *J. Am. Chem. Soc*., **2010**, *132*(35), 12170
[8] Wang Y. J., Wilkinson D. P., Zhang J., *Chem. Rev*., **2011**, *111*(12), 7625
[9] Guo S. J., Zhang S., Sun S. H., *Angew. Chem. Int. Ed*., **2013**, *52*(33), 8526
[10] Gewirth A. A.,Thorum M. S., *Inorg. Chem.*, **2010**, *49*(8), 3557
[11] Choe J. E., You J. M., Yun M., Lee K., Ahmed M. S., Üstündag Z., Jeon S., *J. Nanosci. Nanotechnol.*, **2015**, *15*(8), 5684
[12] Lee K., Ahmed M. S., Jeon S., *J. Electrochem. Soc.*, **2015**, *162*(1), F1
[13] Lu Y., Chen W., *J. Power Sources*, **2012**, *197*, 107
[14] Zhao D. J., Ma S. Y., *Chem. Res. Chinese Universities*, **2015**, *31*(3), 447
[15] Jiang H. J., Wang F. B., Gao Y., Xing W., Shi B. C., Feng Y. Y., Yang H., Lu T. H., *Chem. Res. Chinese Universities*, **2003**, *19*(1), 54
[16] Jeong E., Ahmed M. S., Jeong H., Lee E., Jeon S., *Bull. Korean Chem. Soc.*, **2011**, *32*(3), 800
[17] Wiley B., Sun Y., Xia Y., *Acc. Chem. Res.*, **2007**, *40*(10), 1067
[18] Demarconnay L., Coutanceau C., Leger J. M., *Electrochim. Acta*, **2004**, *49*(25), 4513
[19] Blizanac B. B., Ross P. N.,Markovic N. M., *J. Phys. Chem. B*, **2006**, *110*(10), 4735
[20] Blizanac B. B., Ross P. N., Markovic N. M., *Electrochim. Acta*, **2007**, *52*(6), 2264
[21] Ahern A. J., Nagle L. C., Burke L. D., *J. Solid State Electrochem.*, **2002**, *6*(7), 451
[22] Chatenet M., Genies-Bultel L., Aurousseau M., Durand R., Andolfatto F., *J. Appl. Electrochem.*, **2002**, *32*(10), 1131
[23] Kou T. Y., Li D. W., Zhang C., Zhang Z. H., Yang H., *J. Mol. Catal. A: Chem.*, **2014**, *382*, 55
[24] Singh P., Buttry D. A., *J. Phys. Chem. C*, **2012**, *116*(19), 10656
[25] Guo S., Zhang X., Zhu W., He K., Su D., Mendoza-Garcia A., Ho S. F., Lu G., Sun S., *J. Am. Chem. Soc.*, **2014**, *136*(42), 15026
[26] Herrero E., Buller L. J., Abruna H. D., *Chem. Rev.*, **2001**, *101*(7), 1897
[27] Kirowa-Eisner E., Bonfil Y., Tzur D., Gileadi E., *J. Electroanal. Chem.*, **2003**, *552*, 171
[28] Stevenson K. J., Hatchett D. W., White H. S., *Langmuir*, **1996**, *12*(2), 494
[29] Damjanovic A., Genshaw M. A., Bockris J. O. M., *J. Electrochem. Soc.*, **1967**, *114*, 466
[30] Reyes-Rodriguez J. L., Godinez-Salomon F., Leyva M. A., Solorza-Feria O., *Int. J. Hydrog. Energy*, **2013**, *38*(28), 12634
[31] Bard A. J., Faulkner L. R., *Electrochemical Methods*, Wiley, New York, **1980**
[32] Chatenet M., Aurousseau M., Durand R., Andolfatto F., *J. Electrochem. Soc.*, **2003**, *150*(3), 47
[33] Lima F. H. B., Ticianelli E. A., *Electrochim. Acta*, **2004**, *49*(24), 4091
[34] Sepa D. B., Vojnovic M. V., Vracar L. J. M., Damjanovic A., *Electrochim. Acta*, **1981**, *26*(6), 781
[35] Tammeveski K., Tenno T., Claret J., Ferrater C., *Electrochim. Acta*, **1997**, *42*(19), 893